

# Equivalent Source Technique Processing of Broadband Antenna Measurements

L. Scialacqua<sup>1</sup>, F. Mioc<sup>1</sup>, L. J. Foged<sup>1</sup>, G. Giordanengo<sup>2</sup>, M. Righero<sup>2</sup>, G. Vecchi<sup>3</sup>

<sup>1</sup> Microwave Vision Italy (MVI), Pomezia, Italy, (lucia.scialacqua, lars.foged)@mvg-world.com, francesca@mioc.info

<sup>2</sup> LINKS Foundation, Turin, Italy, (giorgio.giordanengo, marco.righero)@linksfoundation.com

<sup>3</sup> Antenna and EMC Lab, Politecnico di Torino, Italy, giuseppe.vecchi@polito.it

**Abstract**— The equivalent source technique (EQC) has proved to be a useful aid in antenna processing, diagnostics and in the link with Computational ElectroMagnetic Tools (CEM). For broadband frequency antennas or in case of very large number of frequencies, reduction of the number of frequency points to be computed is a desirable feature, to significantly limit the global computational time. In recent applications this is a realistic need, since antennas are present in almost all commercial products, operating on a large set of frequency bands, and exhibiting a wide variety of pattern types. Therefore, they need to be analysed on a relevant number of frequency points, to finally check compliance with standards. For this purpose, in case of multifrequency processing, an interpolation technique based on radiation patterns and antenna S-parameters has been implemented in the EQC. In this paper the new implementation is applied and demonstrated on a large band antenna.

**Index Terms**— Antenna measurements, broadband antennas, equivalent currents, integral equations.

## I. INTRODUCTION

Antennas are present nowadays everywhere: in vehicles, roads, domestic appliances, houses, offices, factories, airplanes, satellite communications buildings and military sites. This is just a subset of different possible specific applications and for each of them particular frequency bands have been allocated by standards to guarantee all communication services. To keep up with these different communication needs and applications, antennas are designed to operate on wider frequency bands and sometimes with an adaptable radiation pattern that guarantee the reliability of the communication even in case of complex scenarios. This is relevant to either low frequency band antennas or high frequency band antennas, like devices for EMC applications or 5G devices, respectively. Indeed, antennas for EMC applications need to be tested on a broad frequency ranges (such as 30 MHz to 1 GHz) and based on the normative, the testing should be extended to higher frequencies up to 6 GHz or higher. Instead in 5G devices beamforming antennas are widely used, which are characterized by a high pattern variability. Therefore, a relevant number of measured frequency points are needed to fully characterize the antenna radiation on the entire frequency band. In order to deal with a high number of frequency points and reduce the processing time, an interpolation technique has been introduced in the equivalent

source method (EQC), reported in [1-2] and also [3-5]. When the EQC technique, implemented in [6], is applied on antenna for diagnostics [7-10] or for link with CEM tools [11-13], this new implementation allows a reduction of the computational time, without sacrificing the accuracy of the results.

In this paper the new implementations of the EQC technique is applied to an MVG Dual Ridge Horn SH800, measured on a relevant number of frequency points to demonstrate the enhancements in total computational time and to guarantee the accuracy of the results.

## II. BROADBAND EQUIVALENT SOURCE TECHNIQUE

The method tries to build an interpolator which takes as input the values of a function on a reduced set of frequency points and a larger set of frequency points and gives values of the function on the larger set of frequency points. The algorithm to build such interpolator uses the available Near Field (NF) measurement data on all the frequency band and the S-parameters. It iteratively selects frequency nodes, i.e. frequency points where the equivalent currents should be computed directly and build the interpolator to reconstruct the currents on other frequency points.

## III. DUAL RIDGE HORN SH800

The antenna under test (AUT) is the MVG SH800 dual ridge horn, shown in Fig. 1. The AUT is linearly polarized and has been designed to operate in the frequency band 08-12GHz with stable gain with respect to frequency. The AUT dimensions are  $H \times W \times L = 270 \times 146.2 \times 225$  mm.

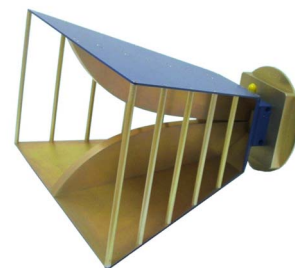


Fig. 1. AUT: MVG dual ridge 800MHz – 12 GHz horn.

A plot of the measured return loss in the full operational frequency band is reported in Fig. 2.

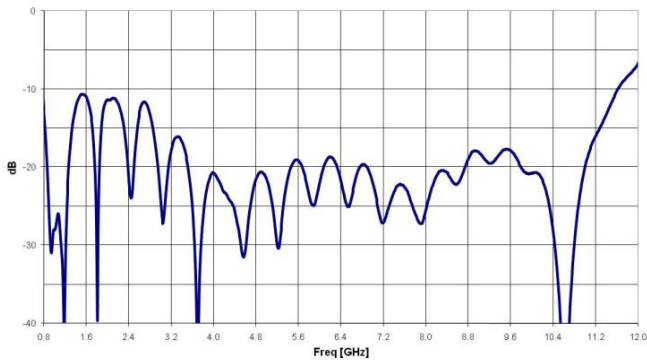


Fig. 2. Measured reflection coefficient [dB] of the SH800 dual ridge horn.

The SH800 has been measured in MVG StarLab (SL) multi-probe spherical NF system in 1.2 – 6.0 GHz frequency range, see Fig. 3. The Horn has been placed in the measurement system with its lower interface offset of 15cm along the vertical axis respect to the centre of the arch.

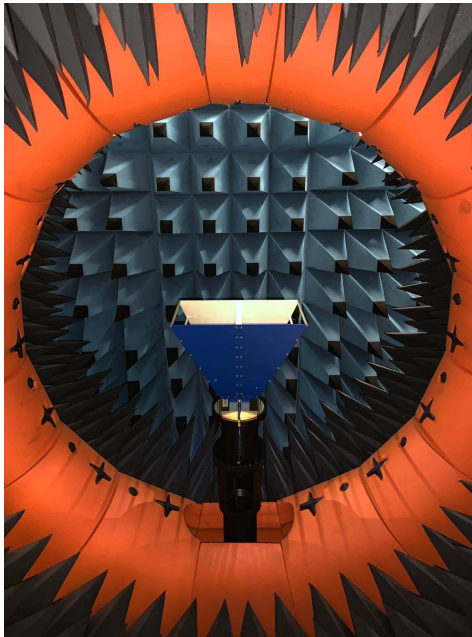


Fig. 3. SH800 dual ridge horn during NF measurement within the MVG SL-18GHz measurement system.

As an example, Co-polar and Cross-polar directivity radiation patterns at 1.0, 2.5, and 6GHz, on the E and H planes are shown in Fig. 4. and Fig. 5, respectively.

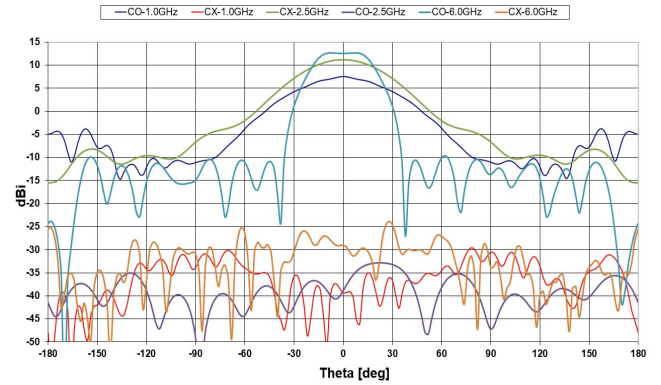


Fig. 4. Directivity radiation pattern of the SH800 dual ridge horn on the E plane @6Hz.

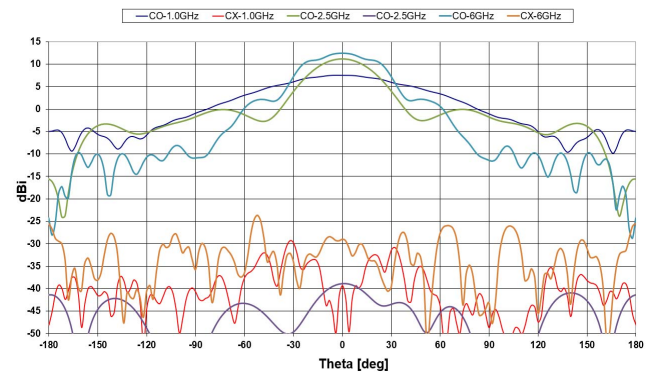


Fig. 5. Directivity radiation pattern of the SH800 dual ridge horn on the H plane @6GHz.

The equivalent current reconstruction technique has been applied to the measured field of the antenna on the 1.2-6GHz frequency band.

#### IV. RESULTS

Results obtained with direct computation at all the 97 frequency points (*reference*) against results obtained with interpolation are compared along the frequency axis. Setting a threshold of 0.005 on the error on the input data (i.e. measured NF data and measured  $S_{11}$ ), the algorithm automatically selects 58 frequency points out of the 97, where the direct computation should be performed, and build the interpolator to reconstruct the data at the missing 39 frequency points. The overall reduction is then around 40%.

The error on the reconstructed NF is shown in Fig. 6 both for the reference case and for the interpolated case. The error is kept lower than 2.5% on the whole band. At 4.1GHz the error in the case with interpolation is the largest.

## V. CONCLUSION

Results concerning the source reconstruction problem for a large number of frequencies, where the currents are computed directly on a reduced set of frequency points and interpolated on the remaining frequency points, are presented. The interpolation algorithm uses all the available measured NF data and the S-parameter to iteratively select important frequency points, where the currents should be computed directly, and to build an interpolator to reconstruct currents at the remaining frequency points.

The interpolation technique allows a reduction of the computed frequency points of around 40%, while the error of reconstruction is kept lower than 2.5% on the whole frequency band. The agreement of the computed equivalent currents between the direct method and the interpolation technique is good. These results demonstrate the enhancements of the EQC method in total computational time and to guarantee the accuracy of the results.

## REFERENCES

- [1] J. A. Quijano and G. Vecchi, "Field and source equivalence in source reconstruction on 3D surfaces," *Prog. Electromagn. Res.*, no. PIER 103, pp. 67–100, 2010.
- [2] J. Araque and G. Vecchi, "Improved-accuracy source reconstruction on arbitrary 3-D surfaces," *IEEE Antennas Wireless Propag. Lett.*, vol. 8, pp. 1046–1049, 2009.
- [3] K. Persson, M. Gustafsson, and G. Kristensson, "Reconstruction and visualization of equivalent currents on a radome using an integral representation formulation," *Progress In Electromagnetics Research B*, vol. 20, pp. 65–90, 2010.
- [4] T. F. Eibert and C. H. Schmidt, "Multilevel fast multipole accelerated inverse equivalent current method employing Rao-Wilton-Glisson discretization of electric and magnetic surface currents," *Antennas and Propagation, IEEE Transactions on*, vol. 57, no. 4, pp. 1178–1185, April 2009.
- [5] Y. Alvarez, F. Las-Heras, and M. Pino, "Reconstruction of equivalent currents distribution over arbitrary three-dimensional surfaces based on integral equation algorithms," *Antennas and Propagation, IEEE Transactions on*, vol. 55, no. 12, pp. 3460–3468, Dec. 2007.
- [6] Insight software website: [https://www.mvg-world.com/en/products/field\\_product\\_family/antenna-measurement-2/insight](https://www.mvg-world.com/en/products/field_product_family/antenna-measurement-2/insight)
- [7] J. L. Araque Quijano, L. Scialacqua, J. Zackrisson, L. J. Foged, M. Sabbadini, G. Vecchi "Suppression of undesired radiated fields based on equivalent currents reconstruction from measured data", *IEEE Antenna and wireless propagation letters*, vol. 10, 2011 p314-317.
- [8] L.J. Foged, L. Scialacqua, F. Saccardi, F. Mioc, J. L. Araque Quijano, G. Vecchi, "Advanced Diagnostics on Array Antennas from Reconstructed Equivalent Current Distribution", 7th European Conference on Antennas and propagation, EuCAP2013, Gothenburg , Sweden, April 8-12, 2013.
- [9] L. J. Foged, A. Giacomini, F. Saccardi, L. Scialacqua, "Analysis of Measurement Probe Spherical Higher Order Modes based on Equivalent Currents", *IEEE Antennas and Propagation Society International Symposium, Fajardo, Puerto Rico*, June 26 - July 1, 2016
- [10] Bo Xu, L. Scialacqua, A. Scannavini, L.J. Foged, Zhinong Ying, T. Bolin, Sailing He, "Antenna Diagnosis and Power Density Measurement of 5G Millimeter-Wave Mobile Terminal Using Inverse Source Technique", 12th European Conference on Antennas and Propagation (EuCAP). London, UK, April 9-13, 2018.
- [11] L. Scialacqua, L. J. Foged, F. Mioc, F. Saccardi, "Link Between Measurement and Simulation Applied to Antenna Scattering and

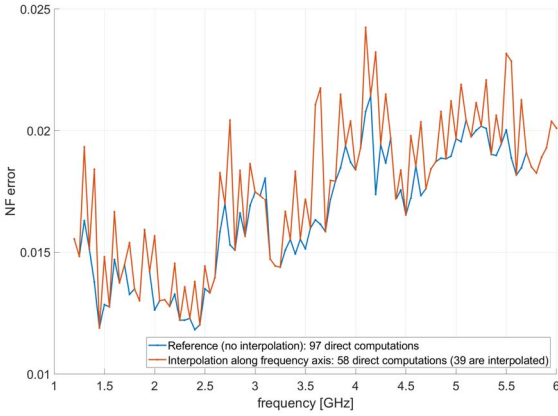


Fig. 6. NF error with direct evaluation and with interpolation along the frequency axis.

Then the equivalent currents are compared at 4.1 GHz. Fig. 7 shows the surface electric current obtained with direct computation on the left panel and the currents obtained with interpolation on the right panel. Fig. 8 shows instead the distribution of the magnetic currents with direct computation on the left panel and the currents obtained with interpolation on the right panel.

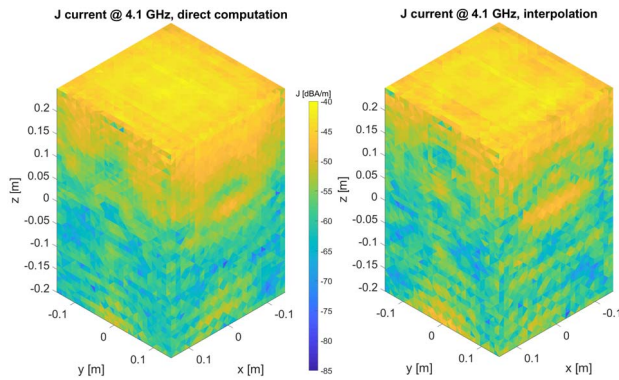


Fig. 7. Surface electric current amplitude [dBA/m] at 4.1 GHz (where the NF error is the largest). Left panel: reference; Right panel: obtained with interpolation

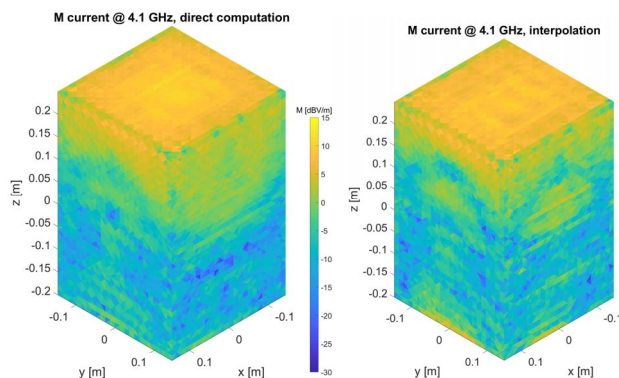


Fig. 8. Surface magnetic amplitude [dBV/m] current at 4.1 GHz (where the NF error is the largest). Left panel: reference; Right panel: obtained with interpolation.

Placement Problems”, 11th European Conference on Antennas and Propagation (EuCAP). Paris, France, March 19-24, 2017.

- [12] L. J. Foged, L. Scialacqua, F. Saccardi, F. Mioc “Measurements as Enhancement of Numerical Simulation For Challenging Antennas”, EUCAP 2015 April 12-17, 2015.
- [13] L. J. Foged, L. Scialacqua, F. Saccardi, F. Mioc, D. Tallini, E. Leroux, U. Becker, J. L. Araque Quijano, G. Vecchi, “Bringing Numerical Simulation and Antenna Measurements Together”, IEEE Antennas and Propagation Society International Symposium, July 6-11, 2014.